

# DISPERSED OXIDES INFLUENCE ON THE KINETICS OF THE WELD METAL STRUCTURAL TRANSFORMATIONS

V.V. Holovko, V.A. Kostin, V.V. Zhukov

E.O. Paton Electric Welding Institute of the NASU

11 Kazymyr Malevych Str., 03150, Kyiv, Ukraine

## ABSTRACT

Research was conducted to study the influence of inoculation of the aluminium, titanium, magnesium, and zirconium dispersed refractory oxides into the weld pool on the modification of the metal structure in low-alloy steel welds. It is shown that the inoculation of refractory oxides into the weld pool increases the temperature at which the bainitic transformation ends and significantly reduces its temperature range. This trend coincides with the size of the wetting angle between the oxide and liquid iron. Increasing the content of inoculants in the weld pool liquid metal from 0.1 to 0.2 % affects the temperatures of the start and finish of the bainitic transformation. Both the start and finish temperatures are increased, that is, the formation of bainite occurs in the higher temperatures region, and the temperature range of this region narrows (the kinetics of transformation increases). An increase in the temperature of the finish of the bainitic transformation and a reduction in its temperature range cause an increase in the acicular ferrite content in the weld metal structure, which corresponds to an increased impact energy level of the weld metal.

**KEYWORDS:** welding, microstructure, dispersed oxides, weld pool inoculation, bainitic transformation

## INTRODUCTION

Improvement of the mechanical properties of welded joints of low-alloy high-strength steels is a relevant problem in the field of welded metal structures. Modern materials science examines the metal modification processes as a leading tool for further development of the scope of low-alloy steel application in manufacture of components, structures and apparatuses designed for operation in extreme conditions. Both the research performed by prominent scientific centers and industrial implementation experience indicate that refractory compound inoculation into the metal melt allows effectively influencing the processes of metal structure formation at the crystallization and recrystallization stages. Application of the currently defined approaches to modification in manufacturing welded metal structures from high-strength low-alloy steels requires expansion of the base of scientific knowledge and concepts as to the influence of dispersed refractory inoculants on development of peritectic processes during formation and development of dendrites in the weld pool, decomposition of the austenite phase with substructure formation and bainitic transformation parameters.

The processes of weld metal modification begin with producing finer austenite grains ( $\gamma$ ), which is a necessary condition, as a large number of ferrite grains ( $\alpha$ ) are formed and grow on  $\gamma$ -grain boundary. In this connection, formation and growth of  $\gamma$ -grains in the matrix, and, hence, also the  $\delta/\gamma$  free energy are of particular interest. During crystallization of low-carbon

steel weld pool the phase transition of delta-ferrite into austenite occurs in a thin hard shell in the immediate vicinity of the meniscus. It is well known that many casting defects form in this region, but still very little is known about the morphological development of this important phase transition.

Modification processes are widely used for improvement of the mechanical properties of both the steels proper, and the metal of welds on these steels. By the nature of metallurgical interaction with the metal it is possible to single out two main types of modifiers: refractory and surface-active. A lot of attention was paid to description of the influence of refractory modifiers, forming refractory insoluble particles with the chemical elements of the metal melt, and promoting heterogeneous formation of nuclei of metal crystallization centers. Results of the performed research are summarized in a number of fundamental studies [1–3].

Much less attention was paid to the influence of surface-active modifiers on the processes of formation of the structure in iron-carbon alloys. They are known to deposit in the form of a thin layer on the surface of metal crystal nuclei in the melt, which causes a reduction in surface energy of the interphases in the melt-solid phase system [4]. It results in an increase in the rate of formation of the crystallization centers, which is associated with reduction of the nucleus critical radius, but the metal crystal growth rate decreases [5]. Such a double effect of surface-active modifiers causes a refinement of the dimensions of the crystallized metal structure [6].

The work gives the results of investigations, which were aimed at expansion of the base of scientific knowledge on the peculiarities of the influence of surface-active modifiers on formation of the weld metal structure. In particular, the influence of wetting of the growing dendrite surface by nonmetallic inclusions on metal structure formation was considered. The data presented in the work will be used in development of new welding consumables, and improvement of the currently available technological processes of low-alloy steel welding.

## STATE OF THE PROBLEM

In the presence of inhomogeneous particles in the melt or unevenness on the dendrite surface the energy required for formation of new phase nuclei, decreases due to interphase tension between the melt, foreign particles and forming nuclei. Crystalline nuclei form on hard particles, which were in the overcooled melt until they reached the critical size. Heterogeneous nucleation usually occurs at crystallization of the steel melt in the weld pool. This is associated with presence of a large number of foreign particles (endogenous and exogenous inclusions). Refractory nonmetallic inclusions can be the center of heterogeneous nucleation of the dendrites and can influence their development, but here we should take into account the widely known negative influence of nonmetallic inclusions on the mechanical properties of the weld metal. The oxides, such as  $\text{Al}_2\text{O}_3$ ,  $\text{MgO}$  and  $\text{TiO}_2$ , are primary nonmetallic forms, which can be present in the weld pool melt.

Investigations of liquid iron wetting in contact with  $\text{Al}_2\text{O}_3$ ,  $\text{MgO}$  and  $\text{TiO}_2$ , showed that in the case of pure iron the wetting angle and the surface tension are within  $105.1\text{--}103^\circ$  and  $1500\text{--}1410$  m·N/m for  $\text{Al}_2\text{O}_3$  substrate, and  $99.2\text{--}90^\circ$  and  $1490\text{--}1270$  m·N/m for  $\text{MgO}$  substrate, respectively. For  $\text{Ti}_2\text{O}_3$  substrate the contact angle is somewhat reduced from  $128.2$  to  $122^\circ$ , and the surface tension has an average value of  $1610$  m·N/m. For cases of  $\text{Al}_2\text{O}_3$ /pure Fe and  $\text{MgO}$ /pure Fe, formation of a reaction layer on the interface of  $\text{FeAl}_2\text{O}_4$  and  $\text{MgO}\text{--}\text{FeO}$  (solid solution), respectively, leads to reduction of the contact angle and the surface tension. In the case of  $\text{Ti}_2\text{O}_3$ /pure Fe the interphase reaction cannot take place. As regards the case of  $\text{Ti}_2\text{O}_3$ /steel, an abrupt reduction in the contact angle and surface tension values are caused by formation of  $\text{Al}_2\text{TiO}_5$  reaction layer [7–9].

Wetting tests, which were conducted between molten alloy Fe–Cr–Ni and  $\text{Al}_2\text{O}_3$ ,  $\text{MgO}$  and  $\text{MgO}\cdot\text{Al}_2\text{O}_3$  oxide substrates in Ar atmosphere at  $1873$  K, allowed determination of the contact angles and interphase energies for each substrate composition. It was determined that molten iron has contact angles of  $114$ ,  $111$

and  $117^\circ$  with  $\text{Al}_2\text{O}_3$ ,  $\text{MgO}$  and  $\text{MgO}\cdot\text{Al}_2\text{O}_3$  substrates, and molten Fe–Cr–Ni alloy has the angles of  $105$ ,  $103$  and  $103^\circ$  with the same substrates, respectively. The difference in the contact angles points to the fact that the wettability between the molten Fe–Cr–Ni alloy and all the three substrates was higher than that between the molten iron and the substrates. The level of interfacial energy of molten iron is equal to  $1862$ ,  $2388$  and  $2781$  m·N/m on  $\text{Al}_2\text{O}_3$ ,  $\text{MgO}$  and  $\text{MgO}\cdot\text{Al}_2\text{O}_3$ , and for molten Fe–Cr–Ni alloy it is  $1513$ ,  $2075$  and  $228$  m·N/m, respectively [7–9]. The differences in the contact angle are attributable to the influence of interfacial energy. The interfacial energy values calculated by the Young's equation were smaller to a greater extent for molten Fe–Cr–Ni alloy with all the substrate types, than those for molten iron. The differences in the interfacial energy level are attributable to higher reactivity of Fe–Cr–Ni alloy at contact with oxide substrates, than that of pure iron.

## THE OBJECTIVE OF THE WORK

was to study the features of the processes of nucleation, growth and development of the precipitated phase morphology during crystallization of the weld pool metal and during phase transformations which are controlled by the free interfacial energy between the refractory oxide particles and the matrix.

## MATERIALS AND RESEARCH METHODOLOGY

Investigation of the influence of refractory  $\text{Al}_2\text{O}_3$ ,  $\text{MgO}$ ,  $\text{TiO}_2$  and  $\text{ZrO}_2$  particles on modification of the structural components of weld metal was performed on deposited metal samples, cut out of the last layer of the metal of a butt weld made with experimental flux-cored wire OERLIKON Fluxcord 35.22 of “metal core” type  $4.0\pm 0.1$  mm in diameter under a layer of ST65 flux to ISO 14171 standard [10]. Physical-chemical parameters of the joints selected for the experiments are given in Table 1.

Samples of the deposited metal were produced by the method of automatic welding using KA-001 welding tractor and KIU-1200 power source. Welding was performed with reverse polarity direct current of  $500\text{--}520$  A, at arc voltage of  $34\text{--}36$  V and welding speed of  $43\pm 1$  m/h. After each pass the butt joint was cooled in air to the temperature of not more than  $120^\circ\text{C}$ . Energy input of welding was equal to  $13\text{--}15$  kJ/cm.

Refractory compound particles of  $200\text{--}500$   $\mu\text{m}$  size were added (inoculated) to the molten metal through the core of  $1.6$  mm flux-cored wire fed to the weld pool in the form of “cold” filler. Filler flux-cored wire was made from a strip of 08Yu grade steel of  $0.8\times 12$  mm size. The charge for the core filling was produced

**Table 1.** Physical and chemical characteristics of the compounds used in the experiments

Compound	$T_{\text{melting}}, ^\circ\text{C}$	Crystalline lattice type	Lattice parameter, nm	$\delta$ -Fe size mismatch, %	Interfacial energy, mJ/m <sup>2</sup>
ZrO <sub>2</sub>	2715	Tetragonal	$a = 3.640, c = 5.152$	1	2863
MgO	2825	FCC	$a = 4.213$	14	2226
TiC	3160		$a = 4.336$	18	884
TiO <sub>2</sub>	1843	Tetragonal	$a = 4.593, c = 2.959$	25	2444
Al <sub>2</sub> O <sub>3</sub>	2044	Rhombohedral	$a = 5.120 (55.25^\circ)$	39	972

from a mixture of iron powder of PZHM grade with inoculants. The inoculant content was equal to 10 % for welds with Al<sub>2</sub>O<sub>3</sub>\*, MgO\*TiO<sub>2</sub>\* and ZrO<sub>2</sub>\* marking and 20 % for welds with Al<sub>2</sub>O<sub>3</sub>\*\*, MgO\*\*, TiO<sub>2</sub>\*\* and ZrO<sub>2</sub>\*\* marking. Strip filling factor was kept in the range of 18–20 %. Schemes of preparation of the butts, welded joint and locations of taking the samples for investigations are given in Figures 1, 2.

Metallographic investigations of the last pass were conducted in optical microscope Neophot 32 on transverse sections of the weld metal, polished and etched in a 2 % solution of nitric acid in alcohol (Nital). The same sections were used for investigation in a scanning electron microscope. Microstructure analysis was conducted in keeping with the requirements of EN ISO 17639 standard [11] and recommendations of IIW [12]. The primary weld structure was studied on polished samples, etched in a boiling saturated solution of sodium picrate (C<sub>6</sub>H<sub>2</sub>(NO<sub>2</sub>)<sub>3</sub>ONa) in water.

Structural parameters were determined with application of MIPAR image analysis software (USA) v.4.2.1, which uses the technology of deep learning with application of artificial intelligence (AI). It allows teaching the software to adapt to analysis of the obtained microphotographs, characterized by different contrast, brightness, dimensions of structural elements and features of the texture, as well as the technique of sample preparation for investigations.

In the latter versions of MIPAR program (higher than v.4.2) a large library of recipes is used to determine the grain size, volume fraction and distribution by phase and inclusion dimensions, as well as the

structure orientation and heterogeneity, texture features, etc. Standard recipes of the MIPAR program were used in the work to determine the size and branching of the grain boundaries in low-alloy steels.

The nature of structural transformations in the alloyed weld metal was studied by simulation of the themodeformational welding cycle (TDWC) in Gleeble 3800 complex, fitted with a high-speed dilatometer. Investigations were performed using a cylindrical samples 6 mm in diameter and 80 mm long, made from deposited metal 20 mm thick. According to the methodology developed at PWI, the samples were heated by a preset program in the vacuum chamber up to a temperature of 1170 °C, and then cooled by different thermal cycles with different cooling rates. The cooling curves corresponded to Newton–Richman dependence and cooling rates of 5; 10; 17; 30; 45 °C/s in the temperature region of 500–600 °C. The cooling parameters of the thermal welding cycles (thermal and time) in the welded joint metal were reproduced quite accurately.

## INVESTIGATION RESULTS

Tables 2–4 give the results of studying the chemical composition, microstructure and results of dilatometric studies of the weld metal, where: WMWI is the weld metal without inoculants.

## INVESTIGATION RESULTS

The movement of the solid/liquid interface at weld pool metal crystallization is characterized by a no-

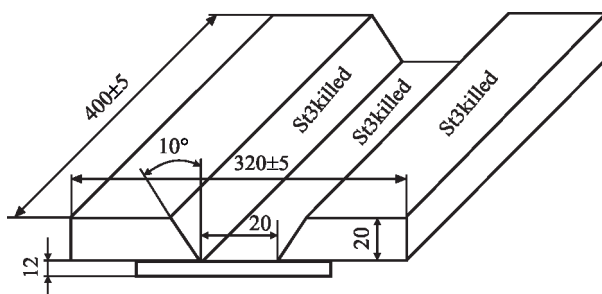


**Figure 1.** Scheme of butt joint preparation to cut out weld metal samples in accordance with ISO 14 [7]

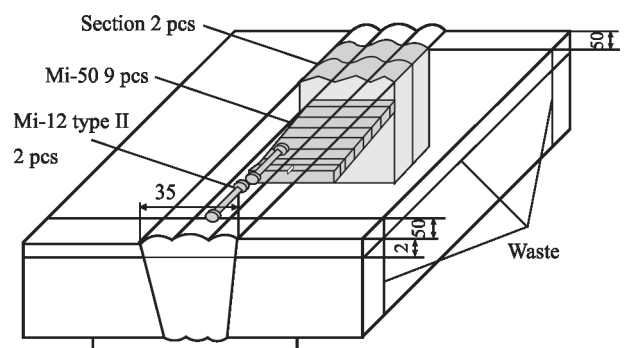


**Figure 2.** Scheme of taking samples for determination of the chemical composition, mechanical properties and structure of the weld metal

Table 2. Chemical composition of the weld metal

Weld	C	Si	Mn	S	P	Cr	Ti	Al	Zr
WMWI	0.053	0.37	1.60	0.008	0.016	0.37	<0.01	~0.004	N/D
Al <sub>2</sub> O <sub>3</sub> <sup>*</sup>	0.060	0.27	1.43	0.014	0.012	0.35	<0.01	0.006	
MgO <sup>*</sup>	0.061	0.42	1.50	0.014	0.012	0.41	<0.01	0.005	
TiO <sub>2</sub> <sup>*</sup>	0.047	0.26	1.48	0.012	0.014	0.40	0.012	0.008	
ZrO <sub>2</sub> <sup>*</sup>	0.061	0.42	1.53	0.017	0.014	0.40	<0.01	0.006	0.007
Al <sub>2</sub> O <sub>3</sub> <sup>**</sup>	0.024	0.26	1.40	0.009	0.014	0.38	0.011	0.009	0.002
MgO <sup>**</sup>	0.029	0.34	1.40	0.015	0.019	0.32	0.018	0.010	0.005
TiO <sub>2</sub> <sup>**</sup>	0.020	0.28	1.40	0.010	0.014	0.30	0.012	0.008	0.001
ZrO <sub>2</sub> <sup>**</sup>	0.024	0.36	1.40	0.015	0.019	0.35	0.014	0.008	0.006

Table 3. Phase fraction and primary crystallite size in weld metal samples

Weld	Phase fraction, %					Primary crystallite size, μm
	AF	PF	Ph	WF	P	
WMWI	95	2.6	2.4	—	—	120–160
Al <sub>2</sub> O <sub>3</sub> <sup>*</sup>	50.4	16.1	28.4	—	5.1	68–77
MgO <sup>*</sup>	84.0	9.3	6.7	—	—	100–125
TiO <sub>2</sub> <sup>*</sup>	91.3	3.7	2.0	3.0	—	115–155
ZrO <sub>2</sub> <sup>*</sup>	84.3	7.3	6.7	1.7	—	50–90
Al <sub>2</sub> O <sub>3</sub> <sup>**</sup>	67.1	13.8	7.2	8.9	3.0	140–200
MgO <sup>**</sup>	73.5	11.0	7.0	5.5	3.0	100–210
TiO <sub>2</sub> <sup>**</sup>	56.5	16.2	15.0	10.7	1.5	60–100
ZrO <sub>2</sub> <sup>**</sup>	55.0	18.0	12.0	12.0	3.0	150–280

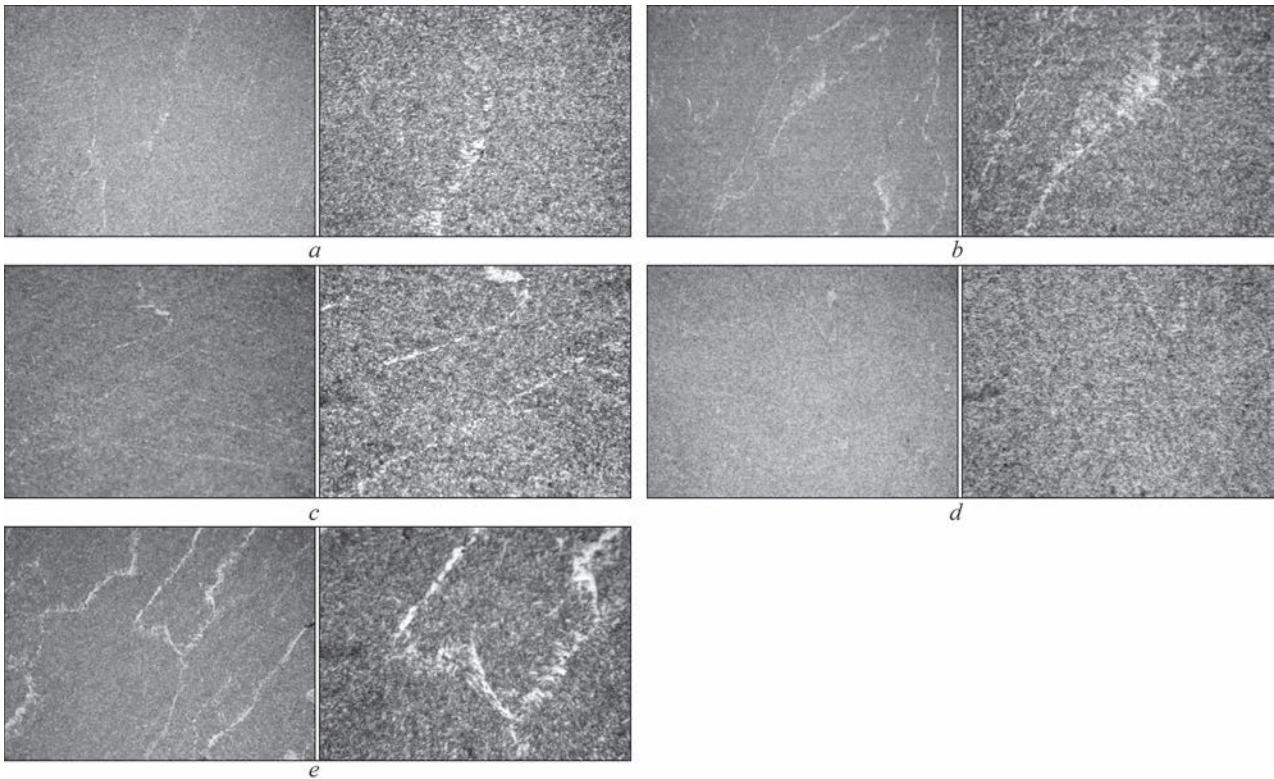
Note. AF — acicular ferrite; PF — polygonal ferrite; Ph — polyhedral ferrite; WF — Widmanstaetten ferrite; P — pearlite.

Table 4. Results of dylatometric analysis of the weld metal

Weld	Ac <sub>3</sub>	Ac <sub>1</sub>	B <sub>s</sub>	B <sub>f</sub>	Δγ	Δα
WMWI	909	718	707	449	191	257
Al <sub>2</sub> O <sub>3</sub> <sup>*</sup>	909	718	749	542	191	206
MgO <sup>*</sup>	907	725	726	497	182	229
TiO <sub>2</sub> <sup>*</sup>	908	722	722	494	187	228
ZrO <sub>2</sub> <sup>*</sup>	905	723	714	487	181	227
Al <sub>2</sub> O <sub>3</sub> <sup>*</sup>	933	725	756	540	208	215
MgO <sup>**</sup>	933	720	766	528	213	238
TiO <sub>2</sub> <sup>**</sup>	933	725	756	540	208	215
ZrO <sub>2</sub> <sup>**</sup>	933	724	766	541	209	224

Note. Ac<sub>3</sub> and Ac<sub>1</sub> are the temperatures of the start and finish of primary austenite decomposition; B<sub>s</sub> and B<sub>f</sub> are the temperatures of the start and finish of the bainitic transformation; Δγ and Δα is the temperature range of primary austenite decomposition and bainitic transformation.





**Figure 3.** Weld metal microstructure with 0.1 % inoculation: *a* — weld metal without inoculations; *b* — MgO\*; *c* — ZrO<sub>2</sub>\*; *d* — Al<sub>2</sub>O<sub>3</sub>\*; *e* — TiO<sub>2</sub>\*; left (×200), right (×500)

ticeable unevenness. In places with a higher level of overcooling the growth of a dendrite in the form of a sharpened peak is initiated. The speed of movement of the dendrite tip in a metal melt and the dendrite size are determined by the surface energy on the solid/liquid interface. Refractory nonmetallic inclusions, which meet with the dendrite tip during its movement in the metal melt, are sorbed on this surface, influencing its energy level. Investigations of the influence of energy distribution anisotropy on the interface on the grain structure formation showed the existence of a reverse dependence between these parameters, namely during crystallization a lowering of the interfacial energy level in the metal promotes an increase in the grain size [7].

The processes of dendrite decomposition are associated with a decrease in the grain boundary energy. Changes in the energy of dendrite grain boundaries have an indirect influence on the distribution of  $\gamma$ -ferrite grain sizes in the metal. Based on comparative analysis of the anisotropy of grain size distribution and anisotropy of grain boundary energy it was shown that there exists a reversible dependence between these two values in polycrystals that envisages the ex-

istence of a relatively larger quantity of grains with low boundary energy, than in the case of high-energy grain boundaries [7, 8]. Thus, a change in the type of the intergranular interlayer in a sample, which leads to a change in the grain boundary energy, also influences the changes in the grain size during transformation. Influence of the presence of refractory oxides in the solid solution on the processes of crystallization and recrystallization of the weld metal was studied on samples prepared by the above described procedure.

Samples of metal microstructure of welds inoculated with MgO, ZrO<sub>2</sub>, Al<sub>2</sub>O<sub>3</sub> and TiO<sub>2</sub> compounds in the amount of 0.1 %, as well as of weld metal without inoculants, are shown in Figure 3.

As one can see from the data given in Figure 4, inoculation of refractory oxides to the weld pool promotes an increase in the temperature of the finish of bainitic transformation and essentially lowers its temperature range. This trend coincides with the influence of the size of wetting angle between the oxide and liquid iron on the transformation temperatures, as was noted above. A certain deviation from such a dependence was noted only for the welds, modified by titanium oxides TiO<sub>2</sub>.

In work [7] such a feature is associated with the fact that for TiO<sub>2</sub> in contact with liquid iron, the melting region forms at the temperature below the melting temperature of pure iron, which is associated with a strong trend to formation of TiO<sub>2</sub>–FeO compounds (solid solution). The kinetics of this process is deter-

**Table 5.** Contact angle of wetting the refractory oxides by the iron melt [9]

Oxide	MgO	ZrO <sub>2</sub>	Al <sub>2</sub> O <sub>3</sub>	TiO <sub>2</sub>
Angle of wetting by Fe-armco	128	123	42	5

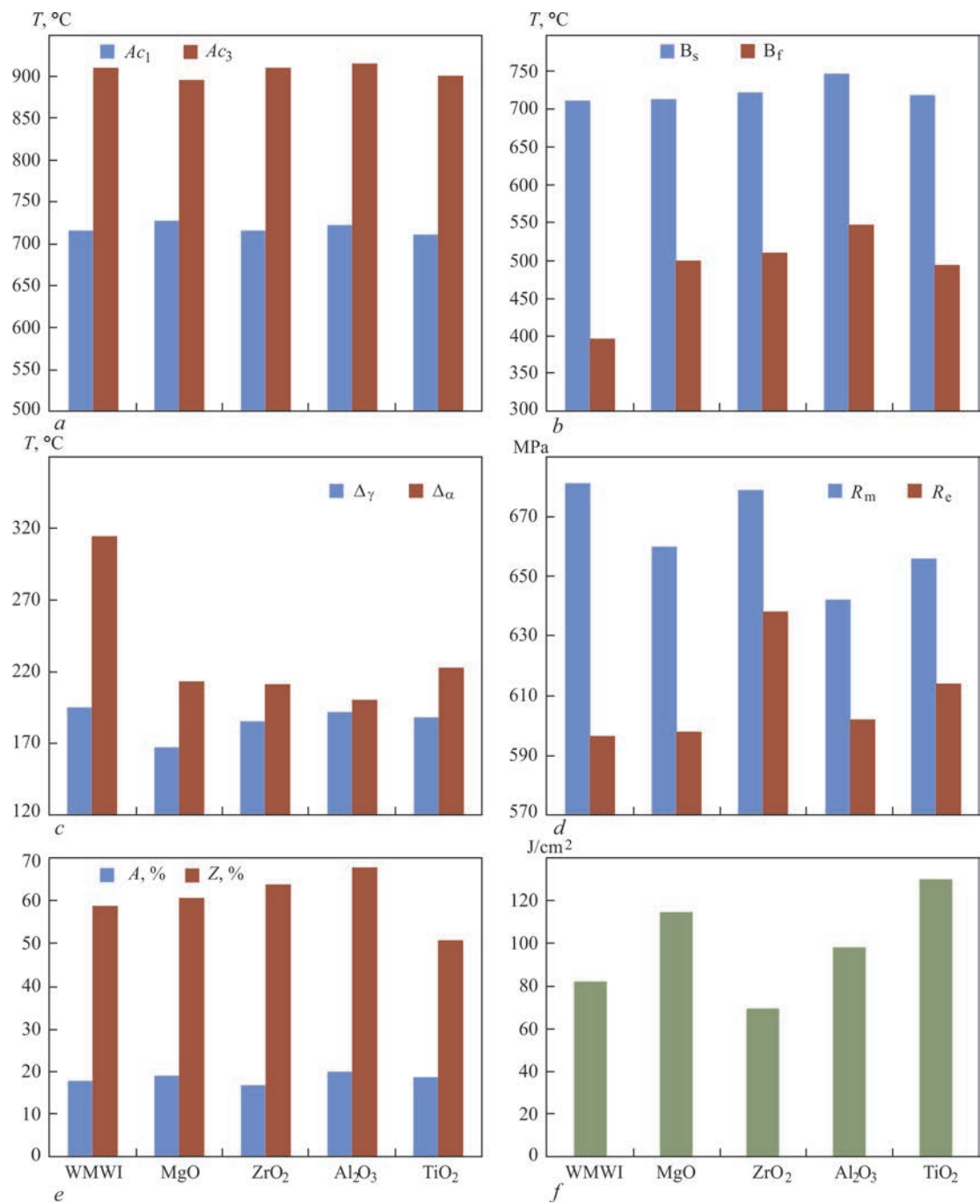


**Figure 4.** Influence of inoculation of 0.1% refractory oxides to the weld pool on structural transformations and mechanical properties of the weld metal: *a* — temperatures of the start ( $Ac_3$ ) and finish ( $Ac_1$ ) of primary austenite decomposition; *b* — temperatures of the start ( $B_s$ ) and finish ( $B_f$ ) of bainitic transformation; *c* — temperature ranges of austenite decomposition ( $\Delta\gamma$ ) and bainitic transformation ( $\Delta\alpha$ ); *d* — ultimate strength ( $R_m$ ) and yield limit ( $R_e$ ) of the weld metal; *e* — relative elongation ( $A$ ) and reduction in area ( $Z$ ) of the weld metal; *f* — impact toughness of weld metal at  $-20^\circ\text{C}$  test temperature

mined by direct reactions between pure iron,  $\text{TiO}_2$  (s) and gaseous oxygen. The main source of oxygen for such a reaction is  $\text{TiO}_2$  decomposition and low partial pressure of oxygen in the solution.

For  $\text{Al}_2\text{O}_3$  and  $\text{MgO}$  which are in contact with liquid iron, formation of the reaction layer of  $\text{FeAl}_2\text{O}$  and  $\text{MgO}\cdot\text{FeO}$  on the interface, accordingly, leads to reduction of the contact angle, but the kinetics of these processes is slower, so that a change in the contact angle can take place with time [8].

Refractory magnesium and zirconium oxides have rather high angles of wetting with liquid iron, unlike titanium and aluminium oxides (Table 5), which readily wet the growing dendrite surface.

Samples of metal microstructure in welds inoculated with  $\text{MgO}$ ,  $\text{ZrO}_2$ ,  $\text{Al}_2\text{O}_3$ , and  $\text{TiO}_2$  compounds in the amount of 0.2 %, are given in Figure 5.

**RESULT ANALYSIS**

Differences in the process of formation of the dendrites, primary and secondary structure of metal in the

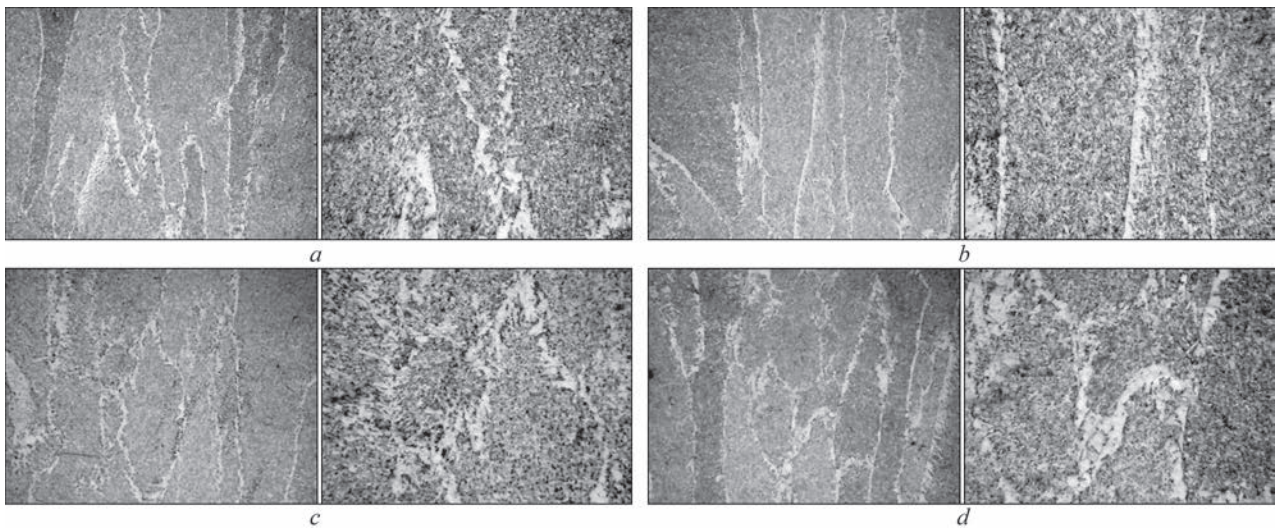


**Figure 5.** Weld metal microstructure with 0.2 % inoculation: *a* —  $\text{MgO}^{**}$ ; *b* —  $\text{ZrO}_2^{**}$ ; *c* —  $\text{Al}_2\text{O}_3^{**}$ ; *d* —  $\text{TiO}_2^{**}$ ; left ( $\times 200$ ), right ( $\times 500$ )

welds inoculated by dispersed particles of refractory compounds, should be related to the features of interphase interaction of the dispersed refractory particles with different morphological formations of the solid phase, appearing in the weld metal at cooling. Weld pool inoculation with refractory particles of magnesium oxide, having rather high angles of wetting with liquid iron, is accompanied by an increase in the temperature of completion of primary crystallization, leading to narrowing of the temperature range of  $\delta \rightarrow \gamma$ -transformation. It results in shifting of the temperatures of the start and finish of the bainitic transformation to higher temperature region, but the temperature range proper becomes narrower (Figure 6).

Weld pool inoculation with refractory particles of zirconium oxide, which also have rather high angles of wetting with liquid iron, is accompanied by an increase in the temperature of completion of primary crystallization, which leads to narrowing of the temperature range of  $\delta \rightarrow \gamma$ -transformation. Similarly, as with the introduction of magnesium oxides, a shifting of the temperatures of the start and finish of bainitic transformation into the higher temperature region occurs, but the temperature range proper becomes narrower (Figure 6).

Increase of the scope of inoculation with magnesium and zirconium oxide particles promotes an increase in the temperature of the start of primary crystallization, that leads to widening of the temperature range of  $\delta \rightarrow \gamma$ -transformation, which is accompanied by a certain increase in the dimensions of prima-

ry crystallites from 100–125  $\mu\text{m}$  in the structure of  $\text{MgO}^*$  weld metal up to 100–210  $\mu\text{m}$  in the structure of  $\text{MgO}^{**}$  weld and from 50–90  $\mu\text{m}$  in the structure of  $\text{ZrO}_2^*$  weld up to 150–280  $\mu\text{m}$  in the structure of  $\text{ZrO}_2^{**}$  weld (Figure 6). A shift in the temperatures of the start and finish of the bainitic transformation into the higher temperature region occurs, but the temperature range proper is expanded, resulting in a decrease in the parameter of integrated perimeter of secondary structure grains from 248737 for the structure of  $\text{MgO}^*$  weld to 225604 in the structure of  $\text{MgO}^{**}$  weld and from 240343 for  $\text{ZrO}_2^*$  weld up to 252681 for  $\text{ZrO}_2^{**}$  weld (Table 6).

Increase in the scopes of addition of  $\text{MgO}$  particles to the weld pool is accompanied by an increase in the temperature range of the bainitic transformation from 229 to 238  $^{\circ}\text{C}$ , while in the case of an increase in the volume of addition of  $\text{ZrO}_2$  particles to the weld pool the range of bainitic transformation remains unchanged (227–224  $^{\circ}\text{C}$ ), which influences preservation of microhardness of polyhedral ferrite on the level of 188–176  $\text{HV}0.1$  at inoculation with  $\text{MgO}$  particles and an increase in microhardness of polyhedral ferrite to the level of 194–210  $\text{HV}0.1$  at inoculation with  $\text{ZrO}_2$  particles.

Interphase interaction on the solid/liquid interface in the presence of refractory  $\text{MgO}$  particles helps inhibit the process of dendrite growth to the dimensions of 100–125  $\mu\text{m}$ , whereas in the presence of  $\text{ZrO}_2$  particles the dendrites grow to the dimensions of

**Table 6.** Integrated perimeter of grain boundaries of the secondary structure of the samples (in pixels)

Inoculant volume, %	$\text{MgO}$	$\text{ZrO}_2$	$\text{Al}_2\text{O}_3$	$\text{TiO}_2$	$\text{SiC}$	$\text{TiC} + \text{Ti}$
0.1	248737	240343	236874	262259	253642	251068
0.2	225604	252681	219168	277395	268201	263162



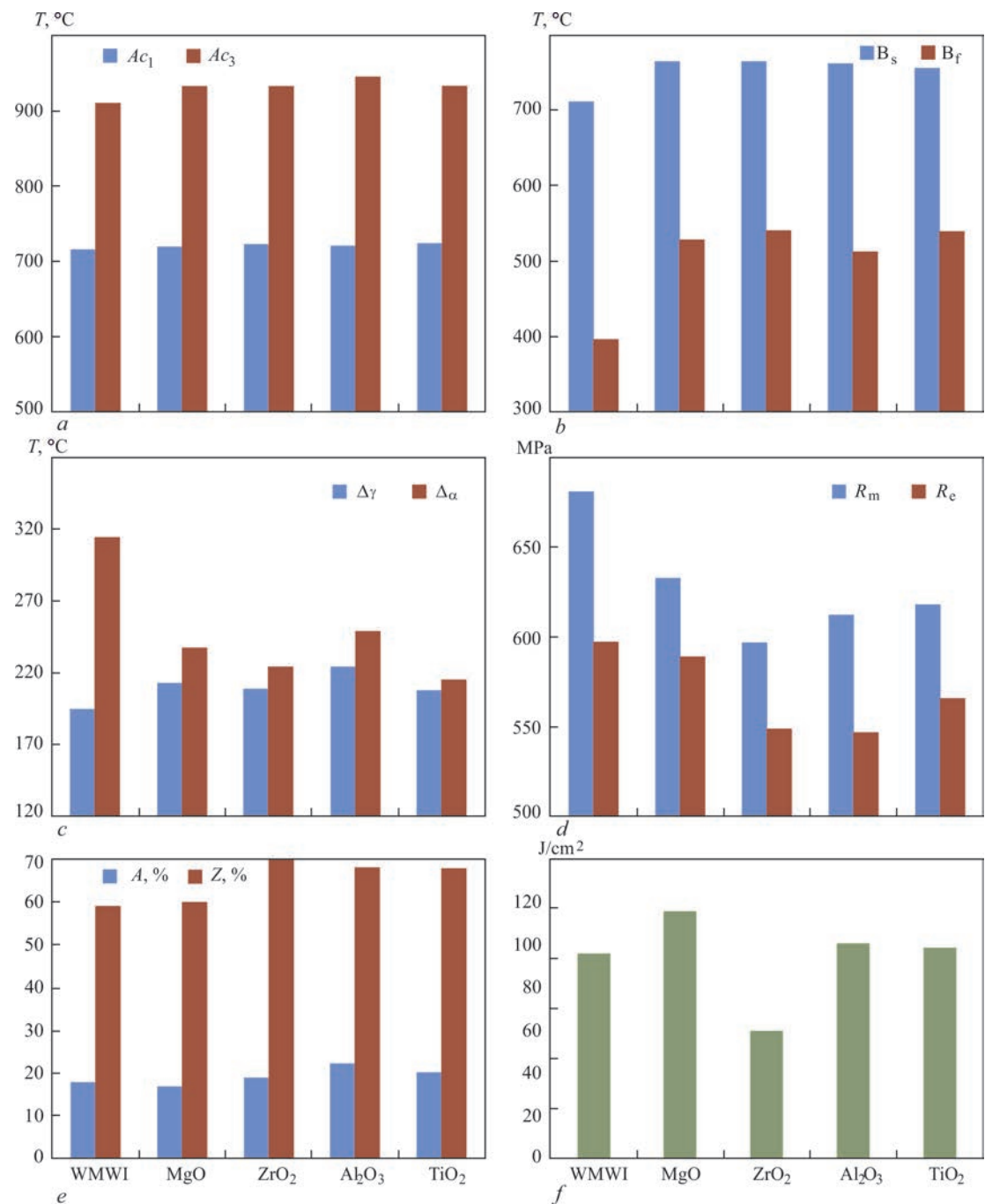


**Figure 6.** Influence of inoculation of 0.2 % refractory oxides to the weld pool on structural transformations and mechanical properties of the weld metal: *a* — temperatures of the start ( $Ac_3$ ) and finish ( $Ac_1$ ) of primary austenite decomposition; *b* — temperatures of the start ( $B_s$ ) and finish ( $B_f$ ) of bainitic transformation; *c* — temperature ranges of austenite decomposition ( $\Delta\gamma$ ) and bainitic transformation ( $\Delta\alpha$ ); *d* — ultimate strength ( $R_m$ ) and yield limit ( $R_e$ ) of weld metal; *e* — relative elongation ( $A$ ) and reduction in area ( $Z$ ) of the weld metal; *f* — impact toughness of weld metal at -20 °C test temperature

150–280  $\mu\text{m}$ , which is attributable to formation of a liquid layer of  $\text{MgO}\cdot\text{FeO}$  composition in the points of contact of the dendrite surface with the inoculant and reduction of the contact angle.

Increase in weld pool inoculation with  $\text{MgO}$  particles promotes both shifting of the bainitic transformation region towards higher temperatures, and increase in the temperature range of the transformation proper to 238 °C. Increase in the content of  $\text{ZrO}_2$  particles promotes an increase in the temperatures of the start

and finish of the bainitic transformation, but does not influence the size of its temperature range (Figure 6).

Preservation of the content of acicular ferrite in the secondary structure of the weld metal at the level of 73–84 % with increase of  $\text{MgO}$  content and 2–5  $\mu\text{m}$  width of the ferrite fringes of the grains, contrary to reduction in acicular ferrite content from 84 to 55 % and increase in the width of the ferrite fringes up to 10  $\mu\text{m}$  with increase of  $\text{ZrO}_2$  particle content, is associated with the changes in the kinetics of the bainitic



transformation processes during inoculation with refractory MgO and ZrO<sub>2</sub> particles (Figures 3, 5).

Changes in the content of acicular ferrite in the metal microstructure (Table 3), branching of the grain boundaries and width of their fringes (Table 6), influenced the lowering of both the strength values from 638 to 549 MPa and impact toughness at 40 °C test temperature from 69 to 37 J/cm<sup>2</sup>.

Increase in the temperature of the finish of bainitic transformation and reduction in its temperature range lead to an increase in the content of acicular ferrite in the weld metal structure (Table 3), which may be related to reduction in carbon diffusion from primary austenite grains during  $\gamma \rightarrow \delta$ -transformation. Increase in the content of ferrite of acicular morphology in the structure corresponds to an increased level of impact energy of the weld metal, and the relatively low value of this parameter for the case of inoculation with zirconium oxide emphasizes the importance of the processes of reaction layer formation on the interface magnesium and aluminium oxides with liquid iron.

At contact of aluminium and titanium oxides a liquid phase of FeAl<sub>2</sub>O<sub>4</sub> and TiO<sub>2</sub>·FeO composition forms at the dendrite growth front, respectively, which influences the process of further formation of the weld metal structure. Increase in the content of aluminium and titanium oxides in the weld pool leads to an increase in the temperature of the start and finish of the primary structure formation, as well as the start and finish of the bainitic transformation (Table 4).

In the metal of welds inoculated with aluminium and titanium oxides, the temperature of the start of the bainitic transformation exceeds that of the finish of primary structure formation, which is accompanied by an increased content of polygonal ferrite and width of the ferrite fringes of secondary structure grains in the weld metal secondary structure. Reduction of the temperature range of  $\gamma \rightarrow \alpha$ -transformation, as well as increase of the temperature of the bainitic transformation end in the metal of these welds inhibits carbon diffusion during recrystallization, which influences an increase in the content of cementite precipitates in the grain body, and an increase in upper bainite content in the metal structure.

Increase in the content of aluminium oxides in the weld metal is accompanied by rising of the temperature of  $\delta \rightarrow \gamma$  and  $\gamma \rightarrow \alpha$ -transformations, leading to an increase in the dimensions of primary crystallites, and of the secondary structure grains (Table 3), reduction in the branching of intergranular boundaries (Table 6) and lowering of the values of weld metal toughness at low temperatures (Table 2).

Increase in the content of titanium oxides in the weld metal is accompanied by an increase in the

temperature range of  $\delta \rightarrow \gamma$ -transformation, with the temperature range of  $\gamma \rightarrow \alpha$ -transformation becoming narrower, which leads to smaller dimensions of primary crystallites and refinement of the ferrite grains (Table 3), and greater branching of the intergranular boundaries (Table 4), but does not result in an increase in the level of metal fracture toughness values (Table 2), which is associated with an increased content of polygonal ferrite and Widmanstaetten ferrite, in keeping with the processes described above.

The data derived as a result of the conducted studies widened the base of scientific knowledge on such phase transformations in steel as restructuring of the crystalline lattice and carbon redistribution between the phases. The features of the influence of these processes on the main types of transformations are shown, namely: ferritic, pearlitic, and bainitic, which successively replace each other at temperature lowering, and on the morphology of the products of decomposition and recrystallization. It is shown that the changes, characteristic for the processes of transformation of the weld structure as a result of pool metal inoculation with the refractory oxides during cooling influence the mechanical properties of the welds.

## CONCLUSIONS

Research was performed, which was aimed at widening the base of scientific knowledge on the features of the influence of surface-active modifiers on formation of the weld metal structure. In particular, the influence of the growing dendrite surface wetting with nonmetallic inclusions on the metal structure formation was considered. Generalization and analysis of the derived data allowed us to formulate the following conclusions.

1. Weld pool inoculation with particles of refractory oxides, having rather high angles of wetting with liquid iron (MgO, ZrO<sub>2</sub>), is accompanied by an increase in the temperature of the end of primary crystallization, leading to narrowing of the temperature range of  $\delta \rightarrow \gamma$ -transformation. During addition of such oxides the temperatures of the start and finish of the bainitic transformation shift towards higher temperature region, but the temperature range proper is narrowed.

2. Interphase interaction on the solid/liquid interface in the presence of refractory MgO particles promotes a deceleration of the process of dendrite growth, which is attributable to formation of a liquid layer of MgO·FeO composition in the points of contact of the dendrite surface with the inoculant and a decrease in the contact angle.

3. Increase in the fraction of inoculated compounds of aluminium, magnesium, titanium and zirconium ox-

ides from 0.1 to 0.2 % influences the temperature of the start and finish of the bainitic transformation. Both the temperature of its start and finish is increased, i.e. bainite formation occurs in the region of higher temperatures, and the temperature range of this region becomes narrower (transformation kinetics is increased).

4. Increase in the temperature of the finish of the bainitic transformation and reduction in its temperature range result in an increase in the acicular ferrite content in the metal structure of welds inoculated with MgO, TiO<sub>2</sub>, ZrO<sub>2</sub> particles, which may be associated with reduced carbon diffusion from primary austenite grains during the  $\gamma \rightarrow \alpha$ -transformation.

## REFERENCES

1. Gubenko, S.I., Parusov, V.V., Derevyanchenko, I.V. (2005) *Nonmetallic inclusions in steel*. Dnipro, ART-PRESS [in Russian].
2. Goldstein, Ya.E., Mizin, V.G. (1956) *Modification and microalloying of cast iron and steel*. Moscow, Metallurgiya [in Russian].
3. Shpis, H.-I. (1971) *Behavior of nonmetallic inclusions in steel during crystallization and deformation*. Moscow, Metallurgiya [in Russian].
4. Popovich, V., Kondir, A., Pleshakov, E. et al. (2009) *Technology of structural materials and materials science. Practical work*. Lviv, Svit [in Ukrainian].
5. Bokshetjn, B.S., Kopetsky, I.V., Shvindlerman, L.S. (1986) *Thermodynamics and kinetics of grain boundaries in metals*. Moscow, Metallurgiya [in Russian].
6. Gulyaev, A.P. (1977) *Metals science*. Moscow, Metallurgiya [in Russian].
7. Rohrer, G.S. (2011) Grain boundary energy anisotropy: A review. *J. Mater. Sci.*, **46**, 5881–5895. DOI: <https://doi.org/10.1007/s10853-011-5677-3>
8. Rohrer, G.S., Anthony, J.G., Rollett, E.D. (2008) A model for the origin of anisotropic grain boundary character distributions in polycrystalline materials. *Applications of Texture Analysis*, **17**, 10. DOI: <https://doi.org/10.1002/9780470444214.ch36>
9. Panasyuk, A.D., Fomenko, V.S., Glebova, H.G. (1986) *Stability of nonmetallic materials in melts*. Kyiv, Naukova Dumka [in Russian].
10. ISO 14171:2008(E): *Welding consumables — Wire electrodes and wire-flux combinations for submerged arc welding of non alloy and fine grain steels — Classification*.
11. ISO 17639:2003: *Destructive tests on welds in metallic materials — Macroscopic and microscopic examination of welds*.
12. IIW Doc. No. IX-1533-88/IXJ-123-87 Revision 2 / June 1988 *Guide to the light microscope examination of ferritic steel weld metals*.

## ORCID

V.V. Holovko: 0000-0002-2117-0864,

V.A. Kostin: 0000-0002-2677-4667,

V.V. Zhukov: 0000-0002-3358-8491

## CONFLICT OF INTEREST

The Authors declare no conflict of interest

## CORRESPONDING AUTHOR

V.V. Holovko

E.O. Paton Electric Welding Institute of the NASU  
11 Kazymyr Malevych Str., 03150, Kyiv, Ukraine.

E-mail: [v\\_golovko@ukr.net](mailto:v_golovko@ukr.net)

## SUGGESTED CITATION

V.V. Holovko, V.A. Kostin, V.V. Zhukov (2025) Dispersed oxides influence on the kinetics of the weld metal structural transformations. *The Paton Welding J.*, **6**, 9–18.

DOI: <https://doi.org/10.37434/tpwj2025.06.02>

## JOURNAL HOME PAGE

<https://patonpublishinghouse.com/eng/journals/tpwj>

Received: 31.10.2024

Received in revised form: 19.03.2025

Accepted: 25.06.2025



# IEEE STEE-2026

## 2026 IEEE 8<sup>TH</sup> INTERNATIONAL CONFERENCE

## ON SMART TECHNOLOGIES IN POWER ENGINEERING AND ELECTRONICS

IEEE Kyiv Polytechnic Week

Igor Sikorsky Kyiv Polytechnic Institute

April 27-30, 2026, Kyiv, Ukraine

<https://stee.ieee.org.ua/>

E-mail: [stee@ieee.org.ua](mailto:stee@ieee.org.ua)

## IMPORTANT DATES

Paper Submission — December 1, 2025

Review — February 15, 2016

Final Paper Submission — March 1, 2026

Acceptance Notification — March 15, 2026

Registration — April 1, 2026

Conference — April 27-30, 2026